

High Fidelity Synthetic SAR Image Generation of a Canonical Target

S. Wong

Defence Research and Development Canada - Ottawa
3701 Carling Ave., Ottawa K1A 0Z4
Canada

silvester.wong@drdc-rddc.gc.ca

ABSTRACT

A 3-dimensional canonical target known as SLICY (Sandia Laboratory Implementation of Cylinders) and the corresponding measured SAR (Synthetic Aperture Radar) image data of SLICY are used to validate the synthetic target image generation process. Computed SAR images of the SLICY target from an electromagnetic code sampled over 360 degrees in azimuth and at two elevation angles are evaluated by comparing against measured images. The results indicate that computed images of high fidelity can be generated if the scattering primitives on the target are correctly identified in the computer-aided design model of the target and this information is properly utilized for computation in the electromagnetic code.

1.0 INTRODUCTION

Achieving accurate computational electromagnetic modeling (CEM) for generating synthetic target signatures in the radar domain has been a challenge. Validation of model simulated results against measurement on benchmark models has always been a goal in the CEM community [1,2,3]. This is especially true in the defence science community where methods for validating simulated radar images of complex targets such as aircraft, ships and ground vehicles with a consistent level of accuracy are highly sought. Simulated SAR (Synthetic Aperture Radar) images can be used in various applications, such as target database compilation in Non-Cooperative Target Recognition (NCTR) and ISR (Intelligence, Surveillance and Reconnaissance) image analysis of targets of interests.

Proper methodology to assess an electromagnetic (EM) code can lead to valuable insights in identifying some of the problems encountered in radar target image simulation and prospective solutions to resolve these problems. A reasonable and logical approach to proper CEM validation is to have a well-defined target model as a benchmark reference for measurements. This benchmark target can be represented by a 3-dimensional computer-aided design (CAD) model for numerical simulation. A target composed of scattering primitives such as flat surface, cylinder, dihedral, trihedral, and elementary cavity provides a well-defined reference. Such a canonical target allows researchers to gain a better understanding of the inner workings of the target signature computational processes.

The objective of this paper is to establish a better understanding of the process of radar image simulation using an EM code. A commercial EM code, FACETS¹ (Frequency Asymptotic Code for Electromagnetic Target Scattering) is used as the computational tool for assessing the numerical simulation process. Measured X-band SAR images of a canonical target known as SLICY (Sandia Laboratory Implementation of Cylinders) in the MSTAR (Moving and Stationary Targets Acquisition and Recognition) are used as benchmark

¹ FACETS is a commercial high-frequency electromagnetic code developed by Thales UK Limited.

High Fidelity Synthetic SAR Image Generation of a Canonical Target

references for comparing with the computed target images. A direct comparison between computed SAR images and measured data provides a sound basis for the validation of the EM code.

2.0 SLICY, A CANONICAL TARGET

SLICY is one of many targets with measured SAR images that are compiled in the MSTAR datasets [4]. An illustration of the SLICY target is shown in Figure 1. According to the MSTAR image provider, the purpose of this target is to provide researchers a means to validate their EM code's algorithm using a well-defined target [5],

“The ‘Slicy’ target is a precisely designed and machined engineering test target containing standard radar reflector primitive shapes such as flat plates, dihedrals, trihedrals, and top hats. The purpose of this target is to allow *Image Understanding* developers the ability to validate the functionality of their algorithm with a simple known target”

2.1 Computer-aided design model of SLICY

SLICY is a vehicle size test target that features a number of scattering primitives. Figure 2 shows the CAD drawings of SLICY. The dimensions of SLICY are 2.75 m in length, 2.445 m in width, and the height of the rectangular box is 0.765 m. The tall cylinder with a close-top is 0.915 m in height with a 0.66 m diameter; the short hollow (open-top) cylinder is 0.458 m in height and a 0.66 m diameter. The inner wall of the short hollow cylinder behaves like a cavity, a special type of scattering primitive. There are also a small trihedral corner reflector, a quarter cylinder and two step-like trihedral corners on SLICY. The scattering primitives on SLICY are identified and illustrated in Figure 3.

3.0 COMPUTATIONAL ELECTROMAGNETIC CODE, FACETS

The FACETS code is capable of generating synthetic SAR images of complex targets such as aircraft, ships and ground vehicles. But it is also a convenient tool to use for investigating the basic image computation process of a simple target. It has a modular algorithmic structure that allows it to facilitate the computation using a combination of different scattering processes, for example, single bounce (flat-plate), double bounce (dihedral), triple bounce (trihedral), edge diffraction (cylinder and top-hat), cavity (hollow cylinder) and shadowing (obstructions between parts on the target). This modular function provides a flexible combination of computing parameters and allows the computed images to be characterized as a function of a number of radar scattering processes available in the code. Thus a well-defined methodology to evaluate simulation-to-measurement validation is available through the use of the FACETS code as a computational and investigative tool.

FACETS computes the SAR image of a target using a number of scattering methods. For example, shooting-and-bouncing ray method is used to illuminate the target and define the target's boundary for scattering computation. Single-bounce and multiple-bounce scatterings on the target due to

High Fidelity Synthetic SAR Image Generation of a Canonical Target

surface-to-surface interaction and reflection (e.g., dihedral and trihedral scattering sites) are computed by a combination of geometrical and physical optics. Edge scattering is handled using various diffraction methods, such as curved surface diffraction, reflection diffraction, edge travelling wave and surface creeping wave. FACETS can also be used to compute scattering from hollow cylinder cavity and more complex structure such as aircraft intake duct with engine components inside the cavity.

FACETS is built with a modular structure for computing various scattering processes. It has a single-bounce scattering algorithm that computes the basic scattering from surface types such as flat plates, cylinders and spheres. FACETS has recognized that it would be difficult to accurately account for, in an automatic manner by the algorithm, the more complex scattering processes such as double-bounce (dihedral), triple-bounce (trihedral), cavity (hollow structure) and diffraction from edges. Thus, FACETS requires all of these scattering processes to be specified for computation; that is, the locations of these types of scattering primitives on the target must be identified and fed into the EM code manually. Graphical illustrations of these scattering primitives are shown in Figure 2. For real-world complex targets such as ships and aircraft, the nominations of all the scattering primitives could be quite labor intensive. However, for a relatively simple canonical target such as SLICY (Figure 1), this is quite manageable. It will be shown that being able to identify and account for all the appropriate scattering types correctly on the target is crucial to the simulation of high fidelity SAR images. It will be demonstrated in the following analysis that this human-assisted algorithmic structure in FACETS can offer some useful and insightful glimpses of what some of the requirements and challenges are for extending the generation of high fidelity simulated SAR images to more complex targets.

4.0 SAR IMAGE SIMULATION AND MEASURED DATA

To analyze the FACETS computations, SAR images of SLICY are computed at two elevation look angles, 15 degrees and 30 degrees, and a full 360-degree coverage in the azimuth direction at X-band radar frequency (9.6 GHz). The computed images are then compared with the measured images of SLICY for validation.

The measured SAR images were collected using the Spotlight SAR mode as part of the MSTAR datasets of ground targets [4, 5]. The SLICY target was stationary; data were captured at a number of depression angles. The Spotlight SAR radar was flown several times around the target, providing multiple 360-degree azimuth coverage at several elevation angles in the measurements. The SAR images of SLICY were cropped from larger scenes of the captured SAR data. The size of the SLICY target image is 54 by 54 pixels. The measured images have down-range and cross-range resolutions of 0.254 m. These correspond to a radar bandwidth of 591 MHz and an angular aperture of 3.5 degrees. The image data are, however, over-sampled to give effective down-range and cross-range pixel spacing of 0.2 m, as described in the header file of each SAR image data file.

For comparative purposes, provision is made so that the 0.2 m pixel spacing is also incorporated in the computed image. This is achieved by using a radar bandwidth of 750 MHz and an angular

High Fidelity Synthetic SAR Image Generation of a Canonical Target

aperture of 4.5 degrees. Thus the computed SAR images have a slightly better spatial resolution. This slightly sharper resolution helps to make it easier to identify various scattering centres on the computed images of SLICY.

The SLICY target is computed as an isolated object in the simulation; that is, there is no ground-plane interaction included in the computation. FACETS computes the single-bounce process for the whole target by default automatically. In addition, locations of the dihedrals, trihedrals, cavity, and edge diffraction are identified from the CAD model and these scattering primitives are computed accordingly. An overall SAR image of the target is then generated from a combination of these scattering processes.

5.0 ANALYSIS OF SIMULATED SAR IMAG

5.1 Comparison between computed SAR images and measured data

Figures 4 and 5 show the comparative results between the computed SAR images using FACETS and the measured images from the MSTAR datasets at 15-degree and 30-degree elevation angles respectively. The images are sampled at a 45-degree interval over a full 360-degree azimuth coverage (at 0, 45, 90, 135, 180, 225, 270, 315 degrees). It can be seen from Figures 4 and 5 that the comparison between the computed and measured images produces good agreement visually for all azimuth angles and at both elevation angles.

Visual inspection of Figures 4 and 5 indicates that all the major scattering sites that are present in the measured images are also present in the computed images. These observations provide a direct qualitative validation of the SAR image computed by FACETS. Although empirical-based comparison may not be seen as objective validation, it is nonetheless universally practiced. Moreover, visual comparison provides a first-order validation that is quite reliable and is generally accepted by the CEM community. The validation results obtained here can be summarized as a consequence of two very basic requirements: 1) a CAD model that is accurate in representing the types of scattering primitives and their locations on the target, 2) a numerical electromagnetic code that can correctly and reliably compute these scattering primitives as single-bounce, double-bounce, triple-bounce or cavity.

Although these two requirements may seem to be obvious and trivial, it is not easy to confirm whether these have actually been met in practice, especially for complex targets such as ships and aircraft. In the case of the SLICY target, a proper and accurate CAD model describing the various scattering primitives and their locations on the target is possible. This may be rather an exception because well-defined scattering primitives are available and there are only a small number of these on SLICY. The geometrical location of a scattering primitive should be within the required resolution of the SAR image. Thus, the higher the image resolution, the smaller is the allowable tolerance on the error of the location of a particular scattering primitive on the target. Furthermore, the type of scattering primitive must be accurately assigned so that single-bounce, double-bounce, triple-bounce and multi-bounce (i.e., cavity) can be properly identified and computed by the

electromagnetic code. It can be seen that if a location in the CAD model where a double-bounce site is misinterpreted as triple-bounce, or vice versa, the computed SAR images will not be consistent and accurate over a range of azimuth and elevation angles when they are compared with measured SAR images. If a double-bounce/triple-bounce site is misinterpreted as single-bounce, a peak could be missing from the computed image. The most difficult case is that of computing a cavity. Depending on the diameter and length of the cavity, the number of bounces that are required to compute a cavity varies. FACETS can handle this quite adequately. One can assign a maximum number of bounces in a cavity to get a fairly accurate output; but that is obtained at a cost of computational time. However, when one assigns a smaller number of bounces to save computing time, the output may not be accurate.

5.2 Analysis of the computed images

The use of the SLICY target provides useful insights into the computational process of synthetic image generation. Figures 6 and 7 show some of the better matches between the computed and the measured SAR images at 15-degree and 30-degree elevation angles respectively. The scattering primitives responsible for the scattered returns are labelled in the computed images. Since FACETS has a modular structure in computing various scattering processes, the contribution of each individual scattering primitive to the SAR image can be verified by having it disabled in the computation. To illustrate this more clearly, Figure 8 shows a sequence of computed SAR images of SLICY at 315-degree azimuth angle, with each of the five scattering primitives disabled, one at a time, in the computations. Figure 8c shows the computed SAR image with all the scattering primitives on SLICY; it serves as the reference image. By disabling each scattering primitive in the image computation, the sequence of images (Figures 8d to 8h) provides a clear demonstration of the contribution from various scattering primitives in composing the overall SAR image.

It is noted from Figures 6 and 7 that the better matches between the computed and measured images are from viewing angles in which SLICY is at a 45-degree viewing angle with respect to the straight edges on the base of the target. That is, the corners of SLICY are pointing towards the radar; these viewing angles correspond to 45, 135, 225 and 315 degrees in azimuth. These target orientations essentially minimize the scattering returns from the long edges and flat surfaces on the sides of the rectangular base of SLICY. Thus the scattering returns that are seen in the SAR images are mainly coming from the dihedrals and trihedrals and the hollow cylinder (cavity) as seen in Figure 8.

The comparison between the measured and computed SAR images with SLICY positioned at edge-on aspect with respect to the radar (e.g., azimuth angles at 0, 90, 180, 270 degrees) are shown in Figures 9 and 10 for elevation angles of 30-degrees and 15-degrees respectively. These comparisons are more complex; the agreements, although still quite good, are not as clean cut and as definitive as those shown in Figures 6 and 7. All the scattered returns from the scattering primitives are seen in both the measured and computed images. The identities of these scattered returns have been verified by the procedure of disabling each of the scattering primitives, one by one as described above. However, there are some extra returns in the measured images that are not present in the corresponding computed images at these edge-on azimuth angles. These extra returns could not be accounted for from physical inspection of the SLICY target model.

High Fidelity Synthetic SAR Image Generation of a Canonical Target

In the 30-degree elevation case (Figure 9), scattered returns from the rectangular base of SLICY are detected in the measured images, although not very strongly. The scattered returns from the base in the computed images are considerably weaker than those in the measured images. This could be due to the fact that there is no ground-target interaction included in the computed images. Whereas, in the case of the measured images, it is reasonable to assume that there may be a dihedral formed between the ground (dielectric) and the sides of the rectangular base, providing some scattered signals.

In the 15-degree elevation images as shown in Figure 10, scattering returns from the sides of the rectangular base are much more pronounced in the measured images. They are also evident in the computed images. Since the computations are done without any ground-target interaction included, the more noticeable returns from the sides of the base in the computed images could be attributed to the smaller elevation angle in the target aspect, making the scattering closer to the specular reflection condition than that in the 30-degree elevation case, and hence has a greater scattering amplitude. There appears to be less spurious scattering returns observed in the measured images at 15-degree elevation (Figure 10). The measured and computed images appear to be in better agreement than those at 30-degree elevation (Figure 9).

Besides the more noticeable scattered returns from the sides of the base, the measured images at these edge-on azimuth angles also pick up spurious scattering returns from the target. These are indicated by the “?” symbol on the measured images in Figures 9 and 10. They occur along the straight edges and at the corner edges of the rectangular base of SLICY as localized point-like spots. These extraneous scattered returns have no obvious corresponding identifiable scattering sites on the target. However, it is generally accepted and expected that there could be imperfections in real measured data, causing various anomalous effects.

5.3 Cavity computations

A notable success of the computed images is the prediction of the scattered returns from the cavity of the short hollow cylinder. The “faint smudge” from the cavity return can be clearly seen in Figures 6, 7, 9 and 10, in both the measured and computed SAR images. The cavity return is indicated in these figures. The cavity return appears at a location on the SAR image that does not correspond physically to where the hollow cylinder is located. This is because the cavity scattering is made up of many bounces along the inner wall of the hollow cylinder due to the large incidence angles of the incident radar rays with respect to the vertical axis of the cylinder. Since the down-range axis of the SAR image corresponds to the differential time delay of the radar rays traveling to-and-fro the radar, the multiple bounces create a longer time delay and hence a displaced spot for the cavity appears on the SAR image. The relative location of the cavity return with respect to the short cylinder is in excellent agreement between the measured and computed images for all azimuth viewing angles; this can be seen in Figures 6, 7, 9 and 10. Moreover, results of the cavity computations have been validated by experimental data obtained from a simple cylinder with a termination flat plate at one end. FACETS-computed scattered radar cross-section returns from cylindrical cavities as a function of incidence angles have been found to be in good agreement with experiments [6].

6.0 CONCLUSIONS

Simulation-to-measurement validation of the computed SAR images of the canonical target SLICY, with well-defined scattering primitives is presented. It is demonstrated that a consistent level of accuracy has been achieved in the computed SAR images by comparing against those from measured data over 360-degree azimuth coverage, and at two target elevation angles. It is shown that the basic scattering processes that are responsible for the scattered returns seen in the measured images of a canonical target can be simulated accurately. By exploiting the modular structure of the electromagnetic code FACETS, it is shown that the functionality of an image generating algorithm can be validated. By identifying the types and locations of the scattering primitives correctly, the SAR image of a target can be computed with high fidelity.

7.0 REFERENCES

- [1] A. Drozd, "Progress on the development of standards and recommended practices for CEM computer modeling and code validation", 2003 IEEE International Symposium on Electro-Magnetic Compatibility, vol.1, pp.313-316 2003.
- [2] W. Coburn, C. Kenyon and C. Le, "Preliminary benchmarking of radar signature prediction codes", Proceedings of the Users Group Conference, pp.262-269, 2005.
- [3] A. M. Raynal, R. Bhalla, H. Ling and V. J. Velton, "An algorithm for target validation using 3-D scattering features", Proceedings of SPIE, vol.6568, pp-1-8, May 2007.
- [4] MSTAR SAR public release datasets, 1997. <http://cis.jhu.edu/data.sets/MSTAR/>
- [5] <https://www.sdms.afrl.af.mil/datasets/mstar/targets.php>
- [6] S. K. Wong, E. Riseborough, G. Duff and K. K. Chan, "Radar Cross-Section Measurements of a Full-Scale Aircraft Duct/Engine Structure", IEEE Transactions on Antennas and Propagation, Vol. 54, No. 8, pp.2436-2441, August 2006.

High Fidelity Synthetic SAR Image Generation of a Canonical Target



Figure 1 A view of the SLICY target (source: MSTAR public release datasets).

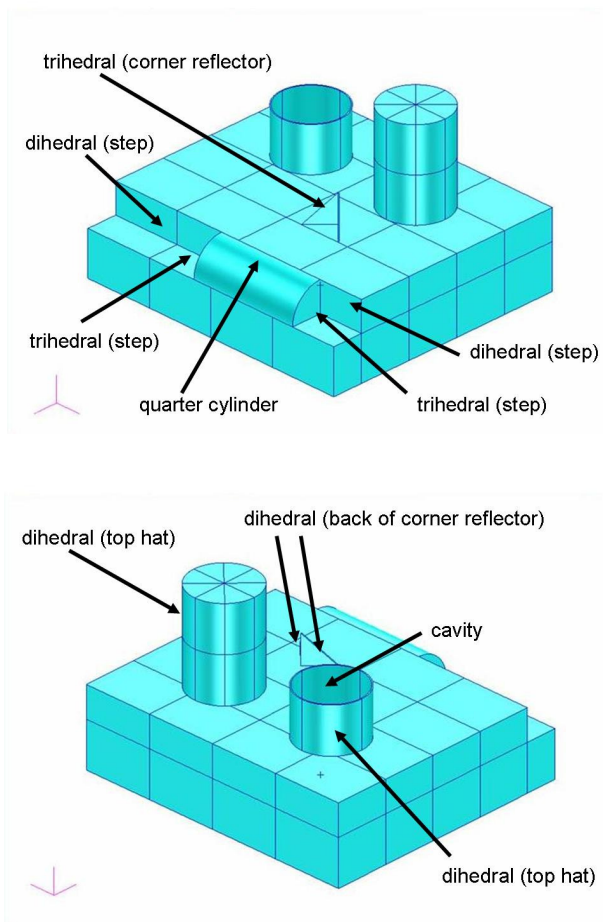


Figure 2 Identification of various scattering primitives on the SLICY CAD model.

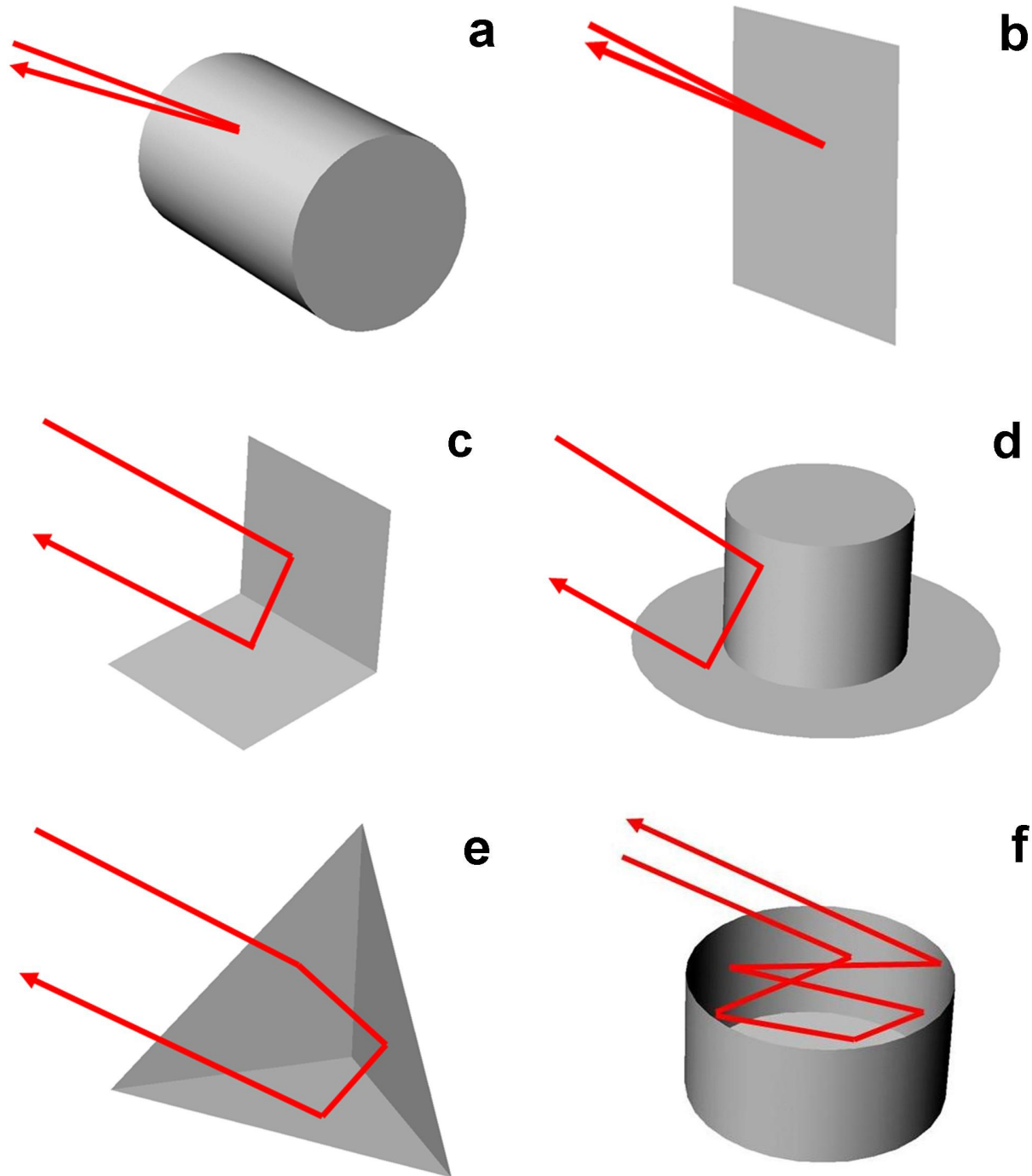


Figure 3 Scattering primitives. a) cylinder, b) flat plate, c) dihedral, d) top-hat (dihedral), e) trihedral, f) cavity.

High Fidelity Synthetic SAR Image Generation of a Canonical Target

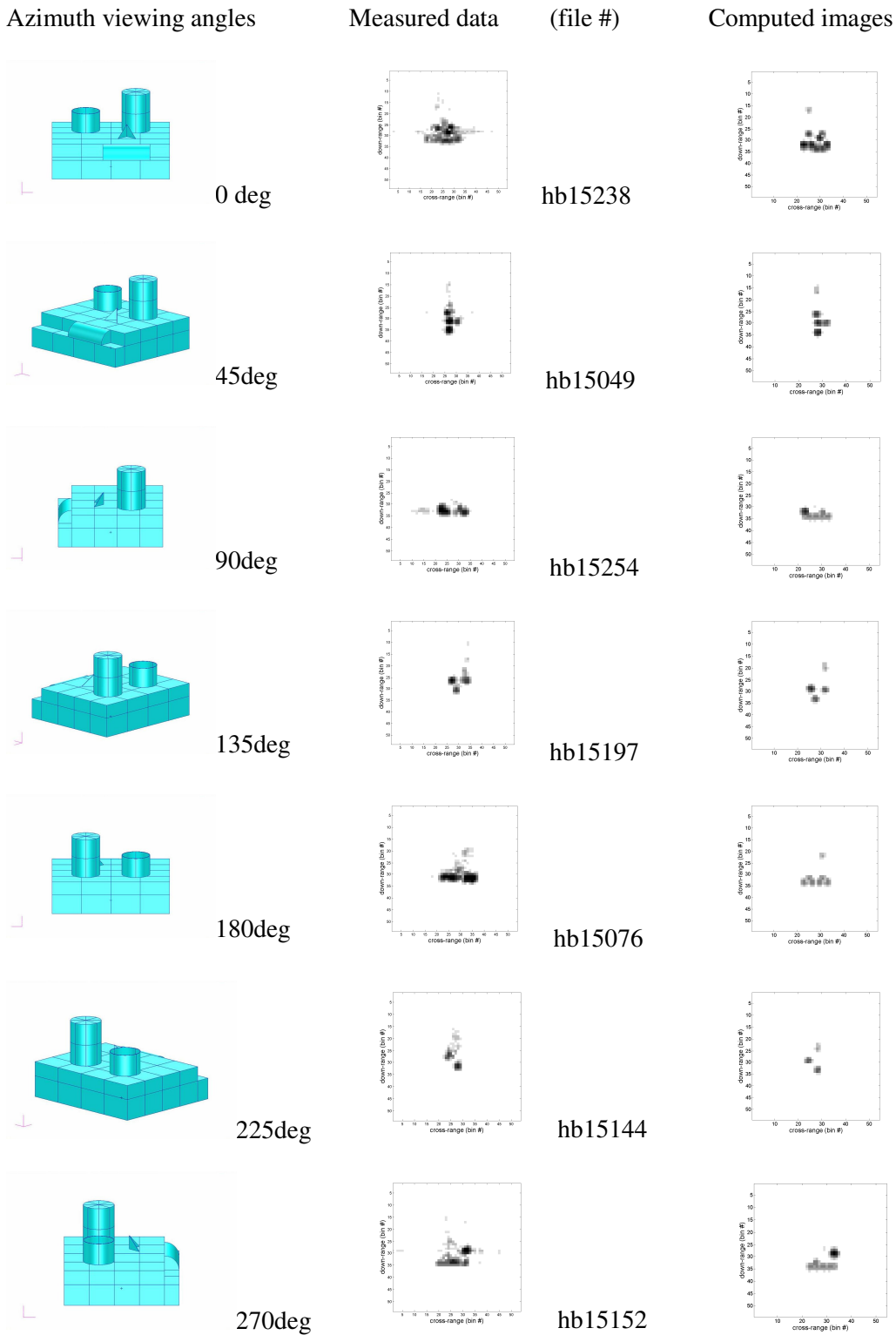


Figure 4 Comparison between computed and measured images at 15-degree elevation angle.

High Fidelity Synthetic SAR Image Generation of a Canonical Target



Figure 5 Comparison between computed and measured images at 30-degree elevation angle.

High Fidelity Synthetic SAR Image Generation of a Canonical Target

Measured data (file #, viewing angle)

Computed images

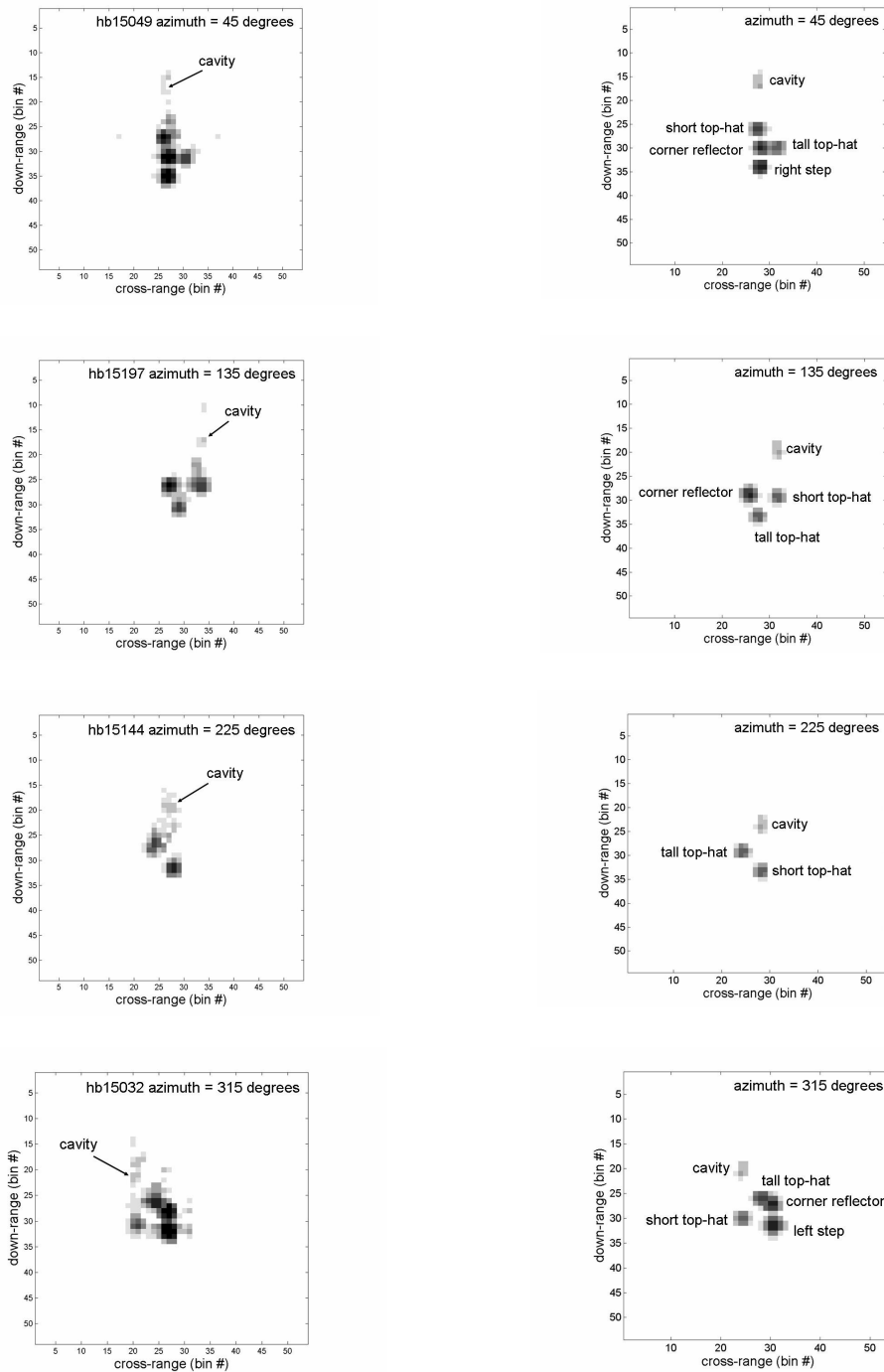


Figure 6 Comparison between measured and computed SAR images at 15-degree elevation angle. Source of the scattered returns are identified and labelled.

High Fidelity Synthetic SAR Image Generation of a Canonical Target

Measured data (file #, viewing angle)

Computed images

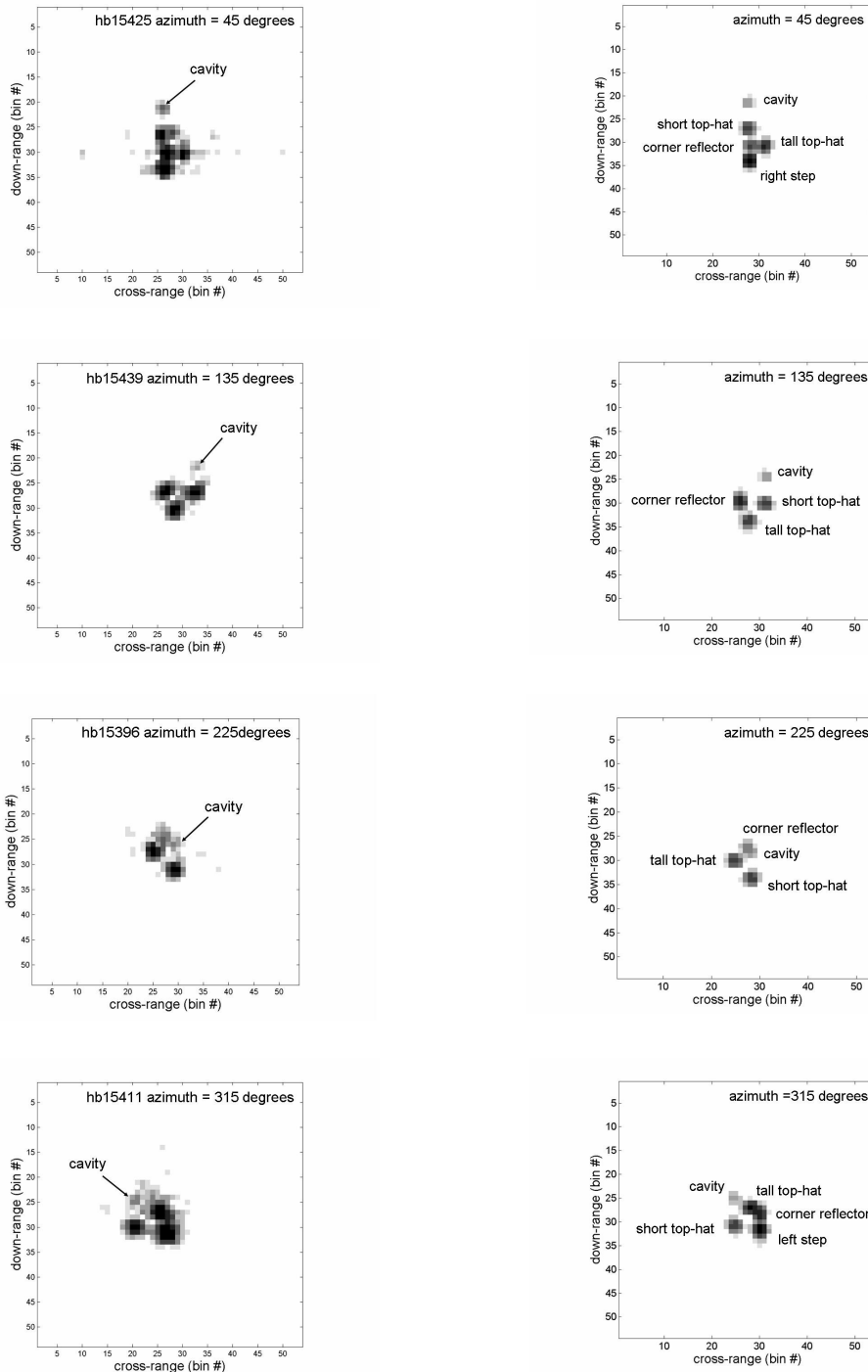


Figure 7 Comparison between measured and computed SAR images at 30-degree elevation angle. Source of the scattered returns are identified and labelled.

High Fidelity Synthetic SAR Image Generation of a Canonical Target

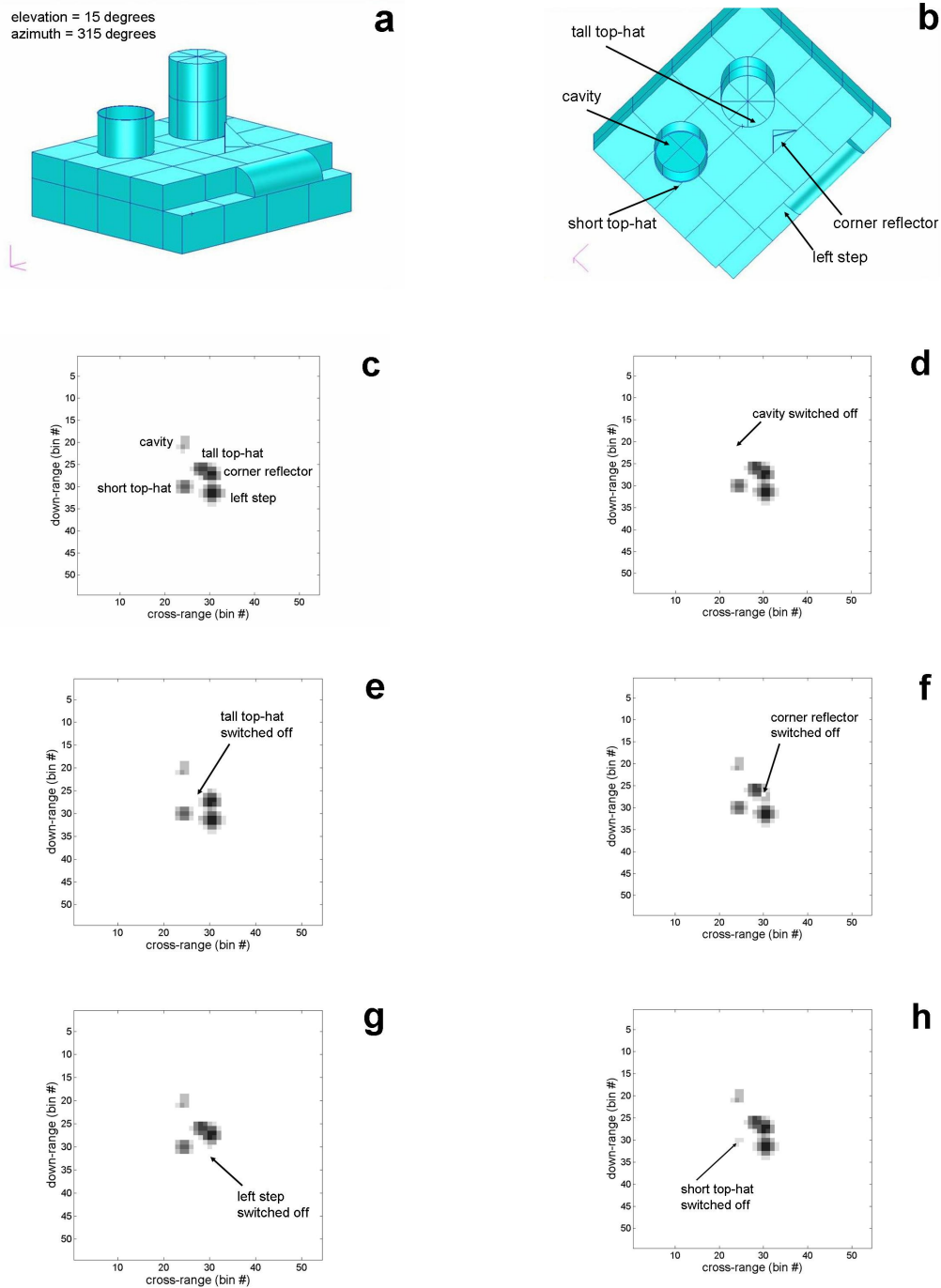


Figure 8 An illustration of contributions from various scattering primitives to the computed SAR images. a) visual view of SLICY as seen by the radar, b) corresponding view of the SAR image projection, c)scattering primitives on SLICY, d) to h) computed SAR images with a different scattering primitive switched off, one at a time.

High Fidelity Synthetic SAR Image Generation of a Canonical Target

Measured data (file #, viewing angle)

Computed images

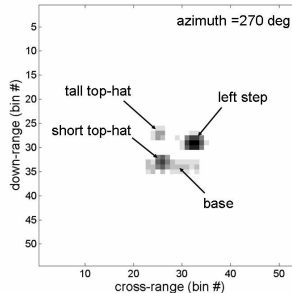
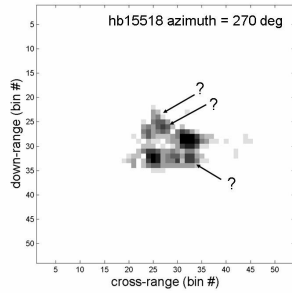
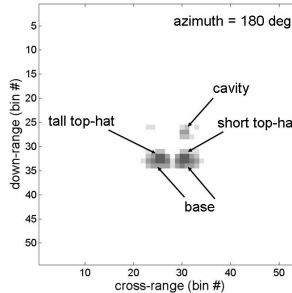
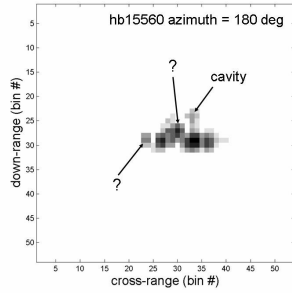
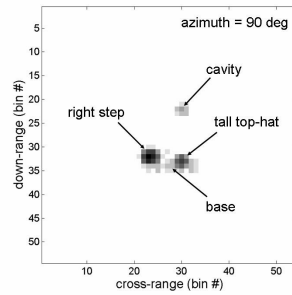
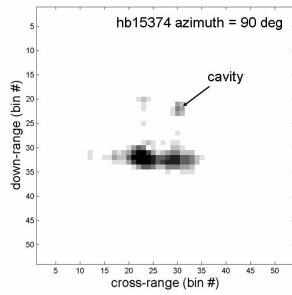
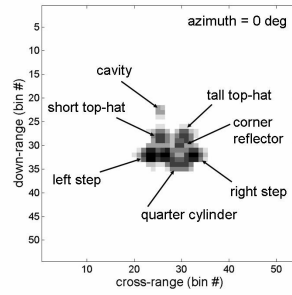
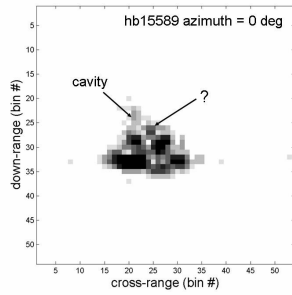


Figure 9 Comparison of SAR images at edge-on aspects at 30-degree elevation angle.

High Fidelity Synthetic SAR Image Generation of a Canonical Target

Measured data (file #, viewing angle)

Computed images

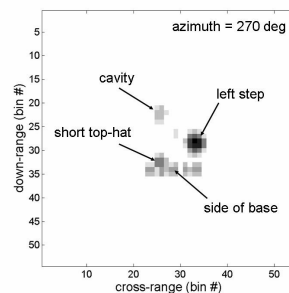
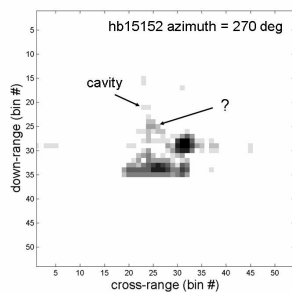
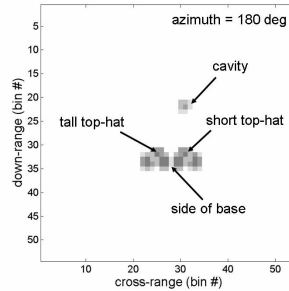
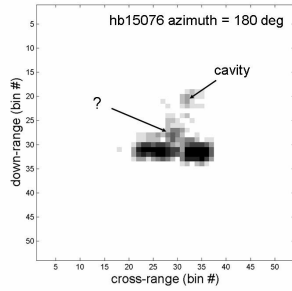
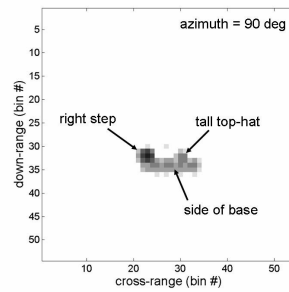
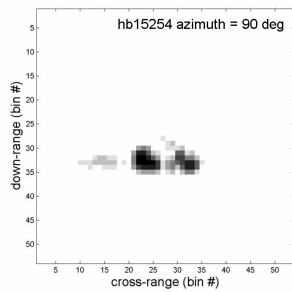
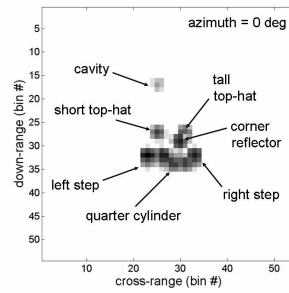
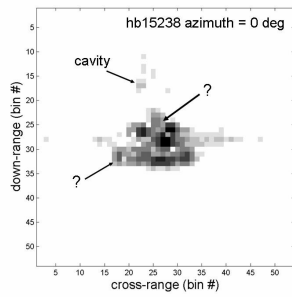


Figure 10 Comparison of SAR images at edge-on aspects at 15-degree elevation angle.